Human Molecular Genetics, 2004, Vol. 13, No. 14 ***1515–1524***
DOI: 10.1093/hmg/ddh159
Advance Access published on May 18, 2004

Normal telomere erosion rates at the single cell level in Werner syndrome fibroblast cells

Duncan M. Baird[†], Terence Davis[†], Jan Rowson, Christopher J. Jones and David Kipling*

Department of Pathology, University of Wales College of Medicine, Heath Park, Cardiff CF14 4XN, Wales, UK

Received April 7, 2004; Revised and Accepted May 11, 2004

The aim of this study was to investigate whether the accelerated replicative senescence seen in Werner syndrome (WS) fibroblasts is due to accelerated telomere loss per cell division. Using single telomere length analysis (STELA) we show that the mean rate of telomere shortening in WS bulk cultures ranges between that of normal fibroblasts [99 bp/population doubling (PD)] and four times that of normal (355 bp/PD). The telomere erosion rate in the fastest eroding strain slows in the later stages of culture to that observed in normal fibroblasts, and appears to be correlated with a reduction in the heterogeneity of the telomere-length distributions. Telomere erosion rates in clones of WS cells are much reduced compared with bulk cultures, as are the variances of the telomere-length distributions. The overall lack of length heterogeneity and the normal erosion rates of the clonal populations are consistent with simple end-replication losses as the major contributor to telomere erosion in WS cells. We propose that telomere dynamics at the single cell level in WS fibroblasts are not significantly different from those in normal fibroblasts, and suggest that the accelerated replicative decline seen in WS fibroblasts does not result from accelerated telomere erosion.

INTRODUCTION

Werner syndrome (WS) is an autosomal recessive disease that displays the premature onset of many age-related phenotypes, including cataracts, skin atrophy, short stature, premature hair-greying and symptoms of age-related diseases such as type II diabetes mellitus, osteoporosis, soft tissue calcification, premature atherosclerosis and neoplasms of mesenchymal origin (1–3). With the exception of central nervous system degeneration, this disease provides a stunning mimicry of the ageing phenotype and is classified as an adult progeria (4).

At a cellular level, WS fibroblasts in culture display limited replicative potentials (5) and have a delayed passage through the S-phase of the cell cycle (6–9). The limited replicative lifespan correlates with an increased rate of exit from the cell cycle compared with normal fibroblasts (10). Analyses of chromosomes from WS cells showed that they have increased numbers of chromosomal aberrations (11,12), including deletions (13), and WS has been classified as a chromosome instability syndrome (14).

The remarkable limitation of replicative potentials of cultured WS fibroblasts has been a major argument in favour of the Hayflick limit having relevance for ageing *in vivo* (15). However, three lines of evidence suggest that the mechanism of cell cycle exit in WS cells may not be comparable with that in senescent cells from control subjects. Firstly, in normal senescent control cultures there is a striking deficiency in the expression of *c*-fos on mitogen stimulation, whereas senescent WS cells exhibit a robust *c*-fos response after such stimulation (16). Secondly, the final telomere lengths in senescent WS cells appear to be longer than in normal controls, even though the rate of shortening appears to be accelerated (17). Telomere shortening is believed to underlie the replicative senescence of control adult dermal fibroblasts (18,19), although there are exceptions including some strains of fetal (20) and mammary (21) fibroblasts. Though it has been shown that ectopic expression of human telomerase can immortalize adult dermal fibroblasts from WS individuals efficiently (22–24), these cells still exhibit slower growth compared with control cells. Thirdly, the lengthening of cell cycle parameters (7–9) and the retarded rate of DNA replication (6) indicate a functional deficit in DNA replication in WS fibroblasts. This could be a consequence of the reduced ability of these cells to process stalled replication forks (9), leading to a proportion of cells with an induced S-phase arrest or delay.

The gene responsible for the WS phenotype encodes a member of the RecQ helicase family (25), but unlike other members of the RecQ family WRNp also encodes a 3′ to 5′

*To whom correspondence should be addressed. Tel: +44 2920744847; Fax: +44 2920744276; Email: kiplingd@cardiff.ac.uk
[†]The authors wish it to be known that, in their opinion, the first two authors should be regarded as joint First Authors.

exonuclease activity (26). WRNp interacts with a range of other proteins involved in DNA metabolism (27) including proteins involved in telomere metabolism. WRNp, in conjunction with the telomere binding protein TRF2 and replication protein A (RPA), may facilitate the unwinding of long tracts of telomeric DNA (28). In addition, WRNp can resolve unusual DNA structures, such as G-tetraplexes, that may occur in the G-rich telomeric strand (29–31) suggesting that WRNp may potentially play a role in modulating telomere dynamics.

A model suggesting that accelerated senescence in WS fibroblasts is a direct consequence of an enhanced rate of telomere loss per cell, resulting in telomere dysfunction, has been formulated (32). This model is supported by data using terminal restriction fragment length analysis that appeared to show an increased rate of telomere erosion in WS cells with ongoing population doubling (PD), when compared with normal cells (17). However, because the rates of telomere erosion for the four WS cultures examined overlapped the rates of erosion seen in normal cells, no firm conclusions could be drawn from these results. Additional data using Epstien–Barr virus-transformed B-lymphoblastoid cells from WS individuals have shown cases where telomere shortening has increased, whereas in other cases the telomere erosion rate has decreased (33). In both of the earlier studies, the cells appeared to reach replicative arrest with telomeres longer than those seen in normal cells, although this has not been confirmed for fibroblasts (23). These data give a rather confused picture for the role of telomere dynamics in the reduced replicative capacity of WS cells.

Therefore, in this work we have used high-resolution length analysis at a single telomere in WS fibroblast strains using a new method for examining telomere lengths single telomere length analysis, (STELA) (34), to formally test the hypothesis that telomere erosion is accelerated in WS cells. Here, we show that it is possible to obtain WS dermal fibroblasts that display normal rates of telomere erosion, and suggest that the accelerated replicative decline seen in WS fibroblasts does not result from accelerated telomere erosion.

RESULTS

Dynamics of erosion of XpYp telomeres in WS cells

WS fibroblasts were passaged serially in culture until the cells ceased dividing, as defined as no increase in cell number over a period of 50 days. Accumulated PDs were monitored with time. Consistent with previous reports (5,10,12,23), both the growth rate and the total number of PDs before the onset of replicative senescence were attenuated considerably when compared with normal fibroblast cultures (data not shown). Using STELA, we have described previously the dynamics of the XpYp telomere during ongoing cell division (CD) in normal fibroblast and derivative clonal cultures. This revealed a mean telomere erosion rate of 86 ± 42 bp/PD (mean ± SD) with a range between 20 and 147 bp/PD (34). Analysis of mean XpYp telomere length using STELA over the life of the WS cultures revealed substantial telomere erosion with ongoing CD [mean 219 bp/PD ($n = 4$), Fig. 1, Table 1], a telomere erosion rate that is significantly ($P < 0.001$, two-tailed z-test) elevated in WS cells compared with normal cells.

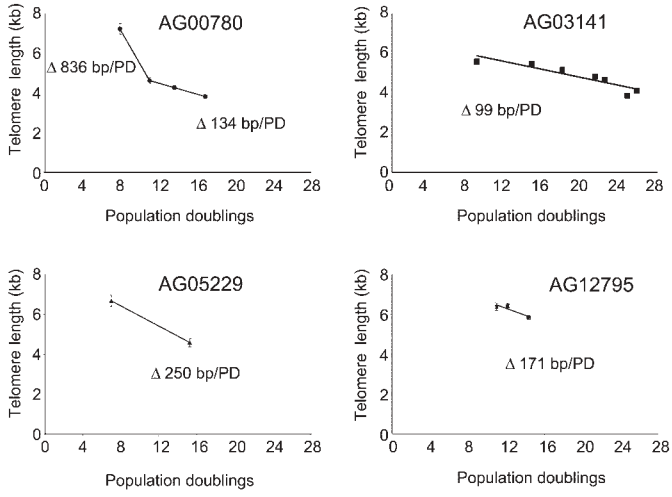

Figure 1. Mean telomere lengths with ongoing CD at the XpYp telomere for each of the WS fibroblast strains studied; telomere loss rates are indicated. The y-axis represents mean XpYp telomere lengths; error bars are ± standard error. The x-axis represents mean PD. The loss rate over the entire lifespan of the AG00780 culture is 355 bp/PD.

Table 1. Mean telomere erosion rates for WS cultures

Cell strain	Maximum PD	Telomere erosion rate (bp/PD)[a]	R^2
AG03141	25.9	99 ($P > 0.69$)	0.85
AG00780	16.8	355 ($P < 0.0001$)	0.80
AG12795	14.4	171 ($P < 0.045$)	0.83
AG05229	15.3	250 ($P < 0.0001$)	1.00
Mean		219 ($P < 0.001$)	

[a]The P-value calculated is the probability that the telomere erosion rates of WS fibroblasts came from the range of erosion rates of normal fibroblast strains [86 ± 42 bp/PD (34)].

However, when the four fibroblast strains were examined individually a different story emerged.

The fibroblast strain AG03141 showed a loss rate of only 99 bp/PD, a rate that is not significantly different ($P > 0.69$) from the mean rate found for telomere loss in normal fibroblast strains (Fig. 1, Table 1).

With AG00780 the situation is more complicated. This cell strain had an average telomere loss rate over the entire life of the culture of 355 bp/PD (about four times that observed in normal bulk fibroblast cultures, Fig. 1, Table 1). However, the vast majority of this loss was accounted for by a loss of 836 bp/PD during the first three PDs of growth (Fig. 1). Thereafter, the rate of loss was only 134 bp/PD over a further six PDs of growth, again not significantly different ($P > 0.23$) from the range for normal cell strains.

Plotting the XpYp telomere-length distributions in AG00780 cells as histograms reveals more detailed information on the dynamics of the telomere erosion in this strain (Fig. 2A). The shape of the distributions changed over time: for example, at PD8 the variance of the distribution is >8 kb, which was accounted for by a significant population (>14%) of cells with telomeres >11 kb in length

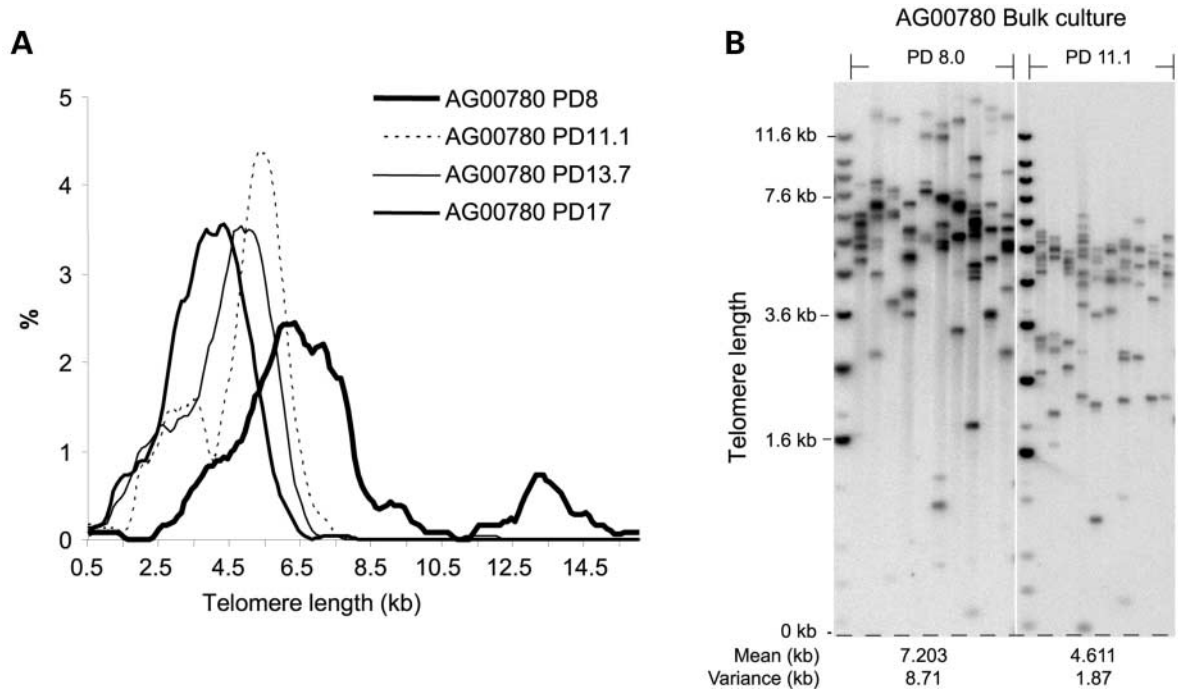

Figure 2. Telomere dynamics of AG00780. (**A**) XpYp telomere-length distributions of AG00780 plotted as a histogram. Fragment sizes were counted into 1 kb bins at 100 bp intervals and plotted as a percentage of the total number of molecules. (**B**) STELA at the XpYp telomere in AG00780 bulk cultures at PD8 and PD11.1. The mean telomere length and the variance are given below the figure. Each DNA sample is subjected to multiple separate telomere PCR reactions (here 10 reactions are shown for each PD point), each containing up to a maximum of 11 amplifiable telomeric molecules. Different reactions are loaded in separate lanes. Each visible band is a single telomeric molecule.

(Fig. 2A and B). This population of large telomeres was virtually absent in later passages (<0.5%), and the variance of the telomere-length distribution had reduced to <2 kb (Fig. 2A and B). A possible explanation for this reduction in heterogeneity is that in the early stages of the culture the majority of the cells were slow growing and/or growth arrested. A plausible explanation is that the cells with telomeres >11 kb represent a clonal lineage that has exhausted its proliferative capacity, presumably as a consequence of telomere erosion at telomeres other than XpYp. Thus, the mean XpYp telomere length in early passages was higher than the modal length. Dilution of this population brings the mean length closer to the modal length in later passages (Fig. 2B). As telomere erosion is determined as a function of the mean telomere length with PD, the rate of erosion will be elevated in the earlier passages. However, even taking these cells into account, the rate of erosion over the first 3 PDs was still high (504 bp/PD). This may be explained if the majority of the growth was due to a few replicatively competent cells that would need to undertake many CDs to achieve 3 PDs for the culture. Support for this is provided by the observation that AG00780 cultures at PD8 had a bromodeoxyuridine (BrdU) labelling index of only 2%, yet this culture achieves 9 PDs of growth, and from the visual inspection of the cultures where patches of dividing cells could be seen clearly on a background of non-growing cells data (not shown).

The AG12795 strain showed a telomere loss rate of 171 bp/PD, which was a little higher than that for normal strains ($P < 0.045$, Fig. 1, Table 1). However, as this strain only achieved 3.4 PD of growth after receipt from the cell repository before entering replicative senescence (at a final total of 14.4 PD), we were unable to examine the dynamics of telomere loss in detail. The observation that these cells at PD11 had a BrdU labelling index of 9% is consistent with telomere loss rates being generated by a subset of cells in the population.

The apparent telomere erosion rate for the AG05229 strain was 250 bp/PD, and the culture achieved 8.3 PD of growth. This was about twice that of the fastest rate of telomere erosion measured for normal cells ($P < 0.0001$, Fig. 1, Table 1). Unfortunately, owing to limited cell numbers only two PD points were obtained for this strain. Thus, the dynamics of telomere erosion between these points are not known.

Allele-specific telomere loss rates

The WS cell strains AG03141 and AG12795 contain heterozygosities in the DNA adjacent to the XpYp telomere that allowed separate analysis of single telomeric alleles. The AT allele has adenine and thymine, at positions −427 and −415, respectively, in the DNA immediately adjacent to the telomere, whereas the GC allele has guanine and cytosine at these positions (35). A detailed analysis of the telomere length of the XpYp alleles in AG03141 at seven PD points revealed a complex pattern of telomere erosion (Fig. 3A). The AT-associated allele lost telomere repeats with a rate of 139 bp/PD, a rate that is within the range of telomere erosion rates observed in normal fibroblast cell cultures ($P > 0.19$). Unexpectedly, the GC-associated telomere showed little apparent change in mean telomere length until the culture reached 21.5 PD; after this point telomere erosion was resumed (Fig. 3A). However, an

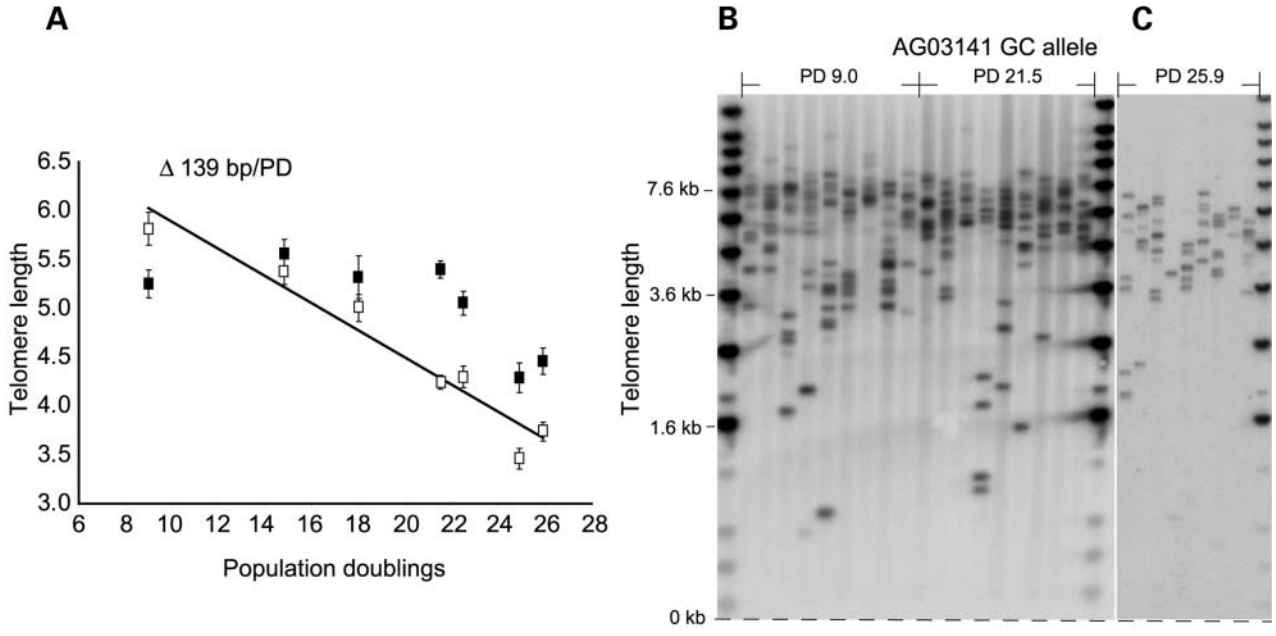

Figure 3. Changes in allele-specific XpYp telomere-length distributions for AG03141 with PD. (**A**) Telomeres linked to the −427G −415C haplotype (GC) are shown as filled squares and those linked to the −427A −415T haplotype (AT) are shown as open squares. A line of best fit is shown for the AT allele but not for the GC allele (telomere erosion rate for the AT allele indicated). XpYp telomere lengths are given as mean ± standard error. (**B**, **C**) STELA of AG03141 GC alleles at PD9 and PD21.5 and AG03141 GC alleles at PD25.9, respectively.

examination of the telomere-length distributions for the GC allele indicated that the mean length at PD9 was low because of the presence of a group of small telomeres (Fig. 3B). The latter have been lost in the subsequent PD points, so the mean actually showed an initial increase. Because of this change in the shape of the distribution we used the modal telomere length, which revealed a telomere loss rate of 39 bp/PD between PD9 and PD21.5, though the subsequent loss appears more rapid. A slow rate of telomere erosion is also found for the GC allele in AG12795 cells (41 bp/PD, $P > 0.27$) compared with the AT allele (158 bp/PD, $P > 0.072$).

Telomere-length heterogeneity

It is clear from STELA data that normal bulk fibroblast cultures have broad heterogeneous telomere-length distributions that become more homogeneous with ongoing CD (34). Single cell clonal cultures, however, have tight homogeneous telomere-length distributions. An interpretation consistent with these data is that the heterogeneity of the telomere-length profile is related to the number of clonal lineages present in a culture. In bulk cultures there are a large number of clonal lineages that reduce with ongoing CD, with perhaps a single clone dominating the senescent cell population (34). Thus, in order to help understand the nature of the growth of WS cultures, we examined the degree of telomere-length heterogeneity in the WS cultures.

The bulk AG03141 culture could be analysed using allele-specific STELA, and thus provided the most detailed data on telomeric heterogeneity. The SDs of the XpYp allele telomere distributions at the initiation of the culture (PD9) were 1.71 and 1.84 for the AT and GC alleles, respectively. These SDs were not significantly different from those of single allele measurements of MRC5 clones ($P > 0.10$, $P > 0.057$), but displayed a significant difference from the SDs of normal bulk populations ($P < 0.021$ and $P < 0.036$, respectively). Similar results are observed for all seven PD points of this culture and for both alleles, with an increasingly significant difference between the AG03141 and the normal bulk populations with ongoing PD. This is illustrated in Figure 4 by a comparison of the telomere distributions for the GC allele in young and senescent MRC5 cells, a clone derived from MRC5 cells and bulk AG03141 cells. The spread of telomere lengths in the bulk population of MRC5 cells is much broader than that seen in the AG03141 cells at a similar telomere length (see MRC5 at PD29 and AG03141 at PD14.8 and PD24.9). The reduced rate of increase in the spread of the AG03141 telomere distributions can readily be explained by a model whereby AG03141 is composed of a lower number of clonal lineages than normal bulk fibroblast populations at all stages of its growth *in vitro*. In the case of AG03141, this was coupled with a normal rate of telomere erosion.

The bulk AG00780 culture could not be analysed in an allele-specific manner, but showed considerable telomere heterogeneity in the early stages of the culture with an SD of 2.95, a value not significantly different from bulk normal cultures ($P > 0.55$, Fig. 2). However, in the later stages the SD had reduced to 1.4, a figure distinct from normal bulk populations but not significantly different from normal clonal cultures ($P > 0.27$). Thus, the number of clonal lineages in AG00780 appeared to be high initially (a point at which there is a high rate of telomere erosion), and reduced in the later stages of growth, coincident with a reduction in the rate of telomere erosion.

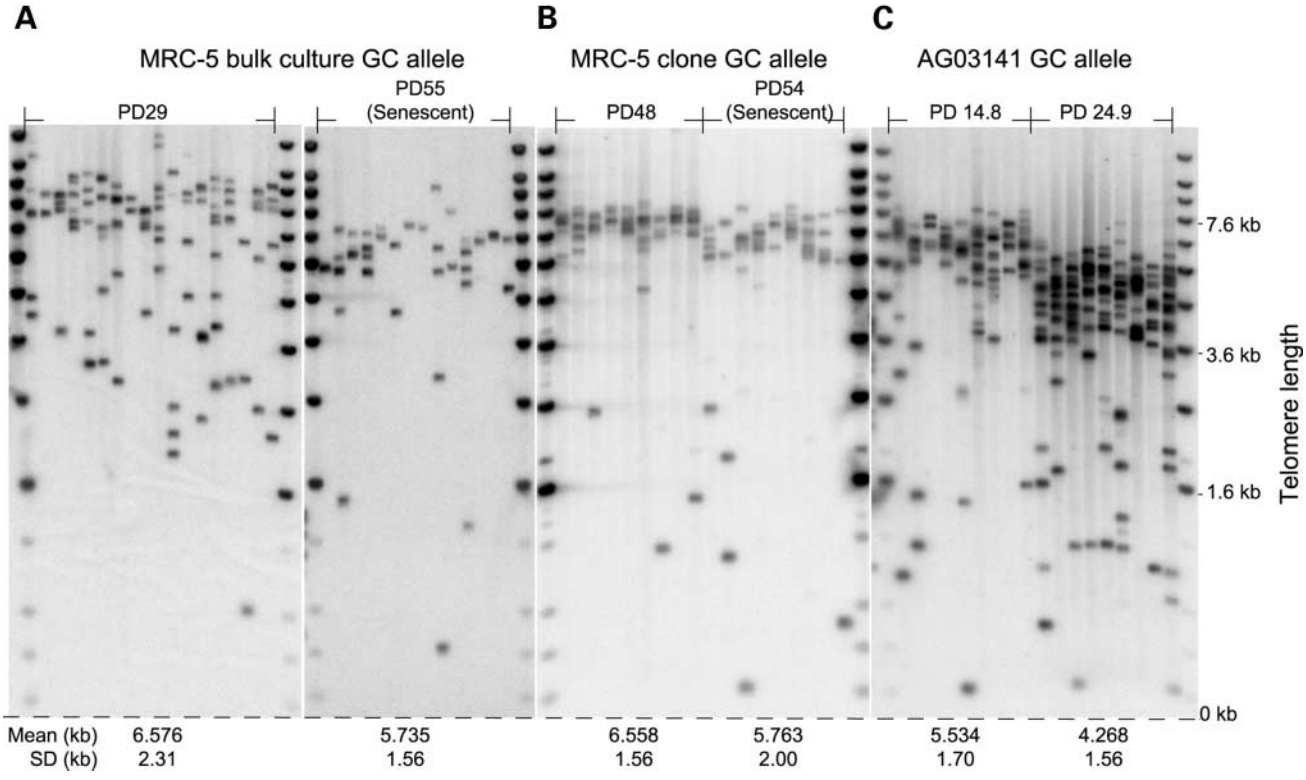

Figure 4. STELA profiles of a MRC5 bulk culture, a clone derived from MRC5 cells, and a bulk culture of AG03141 cells. (**A**) MRC5 GC allele at PD29 and PD55, (**B**) MRC5 clone GC alleles at PD48 and PD54, (**C**) AG03141 GC alleles at PD14.8 and PD24.9. The mean telomere length and the variance are given below the figure.

Allele-specific analysis of the three PD points available in AG12795 revealed a reduction in heterogeneity with ongoing CD, with the SD reducing from 2.53 to 1.57 and 2.74 to 1.91 for the AT and GC alleles, respectively. The early-stage SDs are not significantly different from normal bulk fibroblast cultures ($P > 0.23$ and $P > 0.37$ for the AT and GC alleles, respectively), and in the later stages the SD of the AT allele is not significantly different from normal clonal cultures ($P > 0.16$). However, the SD of the GC allele was slightly higher than normal clonal cultures ($P < 0.045$). Thus, for AG12795 a similar picture emerges as with AG00780, where the culture displayed an apparent decrease in the number of clonal lineages with ongoing CD.

Only two PD points were available for analysis from AG05229. These showed a decrease in SD from 3.13 to 2.40, both of which are not significantly different from normal bulk fibroblast cultures ($P > 0.69$ and $P > 0.16$, respectively). Thus, although this culture may show a reduction in the number of clonal lineages with on-going CD, during the course of its lifespan it did not reach levels significantly different from normal cultures. As with the other cultures at a time when their STELA profiles suggested a high number of clonal lineages, AG05229 displayed a high telomere erosion rate.

Telomere degradation rates in WS clones

Data generated from bulk cultures are confounded by the differing replicative histories and kinetics of the cells within those populations. This can be simplified by clonal analysis, which allows a more detailed understanding of the dynamics of telomere erosion (34). We were unable to obtain clones of WS fibroblasts because these cells grow poorly in highly diluted cultures; however, it was possible to derive clonal cultures following retroviral transduction of a vector that expresses the HPV E6 oncoprotein (36). In these cells, the abrogation of p53 prevented the onset of M1 senescence, resulting in an extended replicative lifespan and a faster growth rate, with the cells entering a second senescence-like state after some 25 PDs (36,37). All of the E6 clones used in this study reached this second proliferative arrest (data not shown). It has been shown that expression of E6 has no direct effect on telomere dynamics in individual cells (38,39). We used E6 simply to allow the outgrowth of colonies with sufficient proliferative potential for at least two points to be sampled by STELA and thus a telomere loss rate to be measured.

We used STELA to analyse WS E6 clones derived from all four WS strains (Table 2). These data revealed tight homogeneous telomere-length distributions (Fig. 5), a result that is typical of that observed in clones from normal fibroblast strains (Fig. 4B). Crucially, all the E6 clonal cultures for all four WS strains showed rates of telomere erosion that were within the range found for normal cell clones (Table 2). This is particularly apparent when comparing the erosion rates of the bulk cultures of AG00780, AG05229 and AG12795 (355, 250 and 171 bp/PD, respectively, Table 1) with their E6

Table 2. Telomere erosion rates for E6-derived WS clones

Clone	PD	Allele	Telomere length (kb)[a]	Telomere loss rate (bp/PD)[b]
AG03141, E6 clone 2	15.3	AT	3.779 ± 0.21	82 ($P > 0.92$)
	21.2	AT	3.289 ± 0.12	
	15.3	GC	5.250 ± 0.29	110 ($P > 0.55$)
	21.2	GC	4.597 ± 0.26	
AG03141, E6 clone 3	14.8	AT	4.119 ± 0.48	114 ($P > 0.48$)
	20.1	AT	3.509 ± 0.17	
	14.8	GC	3.758 ± 0.60	25 ($P > 0.13$)
	20.1	GC	3.626 ± 0.15	
AG03141, E6 clone 4	14.5	AT	5.751 ± 0.39	101 ($P > 0.69$)
	21.3	AT	5.062 ± 0.22	
	14.5	GC	5.084 ± 0.32	80 ($P > 0.84$)
	21.3	GC	4.537 ± 0.26	
AG12795, E6 clone 3	15.1	AT	4.582 ± 0.24	30 ($P > 0.16$)
	16.4	AT	4.543 ± 0.30	
	15.1	GC	5.226 ± 0.22	42 ($P > 0.27$)
	16.4	GC	5.171 ± 0.20	
AG00780, E6 clone 4	19.2	GC	4.500 ± 0.18	102 ($P > 0.69$)
	23.6	GC	4.059 ± 0.15	
AG00780, E6 clone 5	14.5	GC	3.490 ± 0.28	147 ($P > 0.13$)
	16.5	GC	3.197 ± 0.29	
AG05229, E6 clone 6	22.3	AT	3.117 ± 0.17	44 ($P > 0.27$)
	23.5	AT	3.064 ± 0.18	
Mean				80 ($P > 0.84$)

[a]The telomere sizes are given at ±95% confidence interval.
[b]The *P*-value calculated is the probability that the telomere erosion rates of WS fibroblasts came from the range of erosion rates of normal fibroblast strains [86 ± 42 bp/PD (34)].

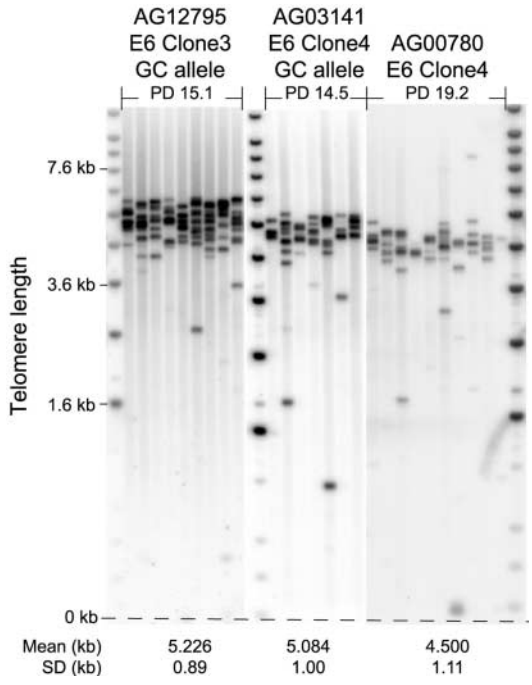

Figure 5. STELA profiles of E6-oncoprotein derived WS clones. A single clone is shown for each of AG00780, AG03141 and AG12795 cells. The mean telomere length and the variance are given below the figure.

clonal derivatives (102–147, 44 and 30–42 bp/PD, respectively, Table 2). Indeed, the erosion rates for the two AG00780 clones were the same as that seen in the latter part of the growth of the bulk population, which provides additional support for our earlier suggestion that this latter growth is also clonal in nature. The mean telomere erosion rates of all the clonal cultures (80 ± 40 bp/PD) was essentially the same as that observed in clones from normal fibroblast strains ($P > 0.84$, Table 2). Thus, irrespective of the WS strain used, these data indicate that it is possible to obtain WS fibroblasts that do not have accelerated telomere erosion rates.

DISCUSSION

This study set out to test the hypothesis that the accelerated replicative senescence that is seen in WS fibroblasts is associated with a fundamental defect in telomere biochemistry and, in turn, an increased rate of telomere erosion per CD. By the use of high resolution XpYp telomere length analysis (34), we examined the dynamics of telomere erosion with ongoing CD in cultures of four strains of WS fibroblasts. These data provide information not only on rates of telomere erosion but also regarding the degree of heterogeneity of the telomere lengths. Previously, we have shown that the telomere-length distribution increases in variance as clones of normal fibroblasts are passaged, an observation in agreement with predictions from models of telomere erosion based on end-replication losses. The variance of the telomere-length distribution thus gives an indirect measure of the number of clonal lineages of a culture, an important issue when interpreting apparent rates of telomere erosion in bulk populations of cells (see below). We studied four independent WS fibroblast strains and analysed both bulk populations and clonal cultures. To produce the latter, we were obliged to study cells expressing HPV E6. However, there are published data that indicate that E6 does not significantly affect telomere erosion rates (38,39), a conclusion supported by our own data (e.g. rates of telomere erosion are unchanged in both AG03141 cells and E6-expressing AG03141 cells, Tables 1 and 2). However, we cannot fully exclude the possibility that E6 expression will affect a pathway involved in telomere maintenance.

The rate of telomere erosion per PD for bulk WS cultures varies from a normal rate to a rate around four times that for normal cells. However, each strain shows a distinctly different behaviour with respect to the dynamics of telomere erosion. The AG03141culture has a telomere erosion rate well within the range seen for clones of normal cells (34). The AG00780 culture shows a very high rate of telomere erosion in the first 3 PDs of growth that converts to a normal rate with ongoing PDs. AG05229 and AG12795 cultures have a high rate of telomere shortening throughout their lifespan, although the data are more limited for these two strains. However, for each of the four strains, the telomere erosion rates in the E6-derived clones are within the range found for normal cell clones (34). Thus, there are circumstances when a normal rate of telomere shortening can be observed for all four of the WS cell strains.

A consistent picture emerges when comparing the telomere erosion rates with the variance of the telomere-length distribution. In each case, when normal rates of telomere erosion are observed in WS cultures, the STELA profile is suggestive

of a culture that is largely clonal in nature. E6-expressing clones and WS cultures at a point when they appear naturally to be clonal show rates of telomere erosion that are not significantly different from clones of wild-type fibroblasts. Studying clones (or clonal cultures) produces the most accurate estimates of telomere erosion rates per CD, and based on these data we conclude that the rate of telomere erosion per CD is unaltered in WS fibroblasts.

Why then do some WS cultures, especially at the beginning of their lifespan, appear to have unusually high rates of telomere erosion? A possible explanation is that there are confounding phenomena in WS, namely, the clonal succession, attenuation and expansion, that are observed in WS fibroblasts (11,12,40–42). This phenotype is displayed by normal fibroblasts, but to a much lower degree (41,43,44). This clonal succession may result in the bulk of WS cell growth resulting from a small number of dividing cells in the population (40,41). Superimposed upon this clonal succession is a more rapid exit from the cell cycle (10). These phenomena acting together lead to an increased rate of change in the mitotic pool, and as a consequence, telomere loss in the bulk population measured as a function of PDs will appear higher than in a normal cell culture, even though the rate of telomere loss per CD is the same. Thus, a 'population doubling' of a bulk WS culture at an early passage would represent many CDs for the growing clones, whereas later passages of the population are dominated by these clones. In this situation, PD estimates would represent an under-estimate of the actual number of CDs, and thus telomere erosion rates would appear artificially high, as they are measured as a function of PDs and not of CDs. There are several aspects of our data that would be consistent with such a model, especially the reduction in telomere length variability that uniquely occurs in WS as erosion rates approach wild-type rates. Our proposed model for the clonal growth of the WS cultures is shown in Figure 6 (for full details see legend). In this model, we suggest that the four WS cultures are at different points in the same process of proceeding from a culture with a high number to a culture with a low number of clonal lineages, which possibly reflect their different replicative histories before explantation.

Our data imply that the accelerated replicative senescence of WS cells is not mediated by an elevated telomere loss rate per CD, in contrast to the model suggested earlier (32). This may appear to contradict previous data reporting an elevated telomere erosion rate in WS cells compared with normal cells as determined by terminal restriction fragment analysis which estimates the mean genome-wide telomere length (17). It should be noted, however, that two of the four WS strains used previously have telomere erosion rates within the range found for normal cells; the other two WS strains had rates approximately twice that for normal cells (17). These authors concluded that, although telomeres may shorten faster, this was unlikely to be responsible for the accelerated replicative decline seen in WS cells. Our data confirm and extend these conclusions, and provide strong evidence that the accelerated replicative decline of a WS culture is not a result of accelerated telomere erosion due to elevated end-replication losses at the single cell level.

We therefore postulate that the accelerated replicative decline seen in WS cells results from a telomere independent

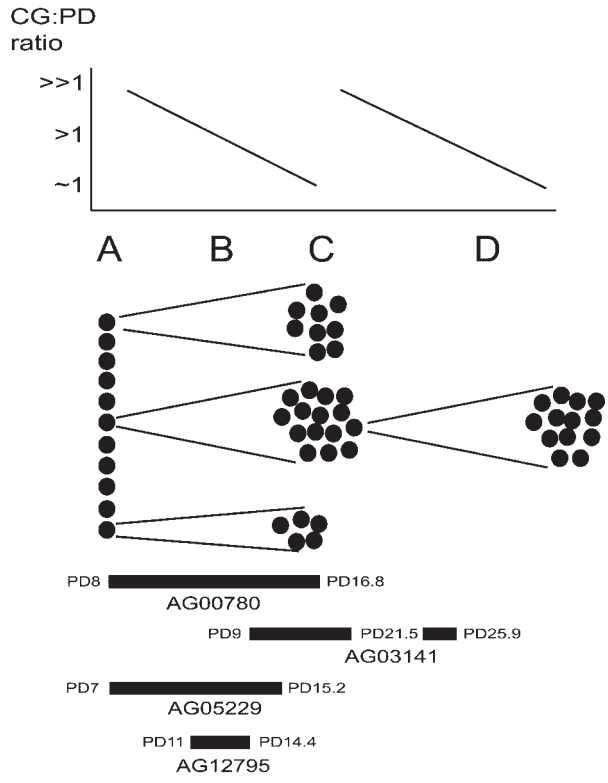

Figure 6. Clonal growth model for WS cultures (adapted from 12,42). Stage A is a culture where the majority of the cells are slow growing and/or growth arrested. At stage B, some cells have a growth advantage and expand into clonal populations (stage C). Most of the cells at late stage C are growth arrested and a second clonal expanse is seen in stage D. The number of clonal lineages of the culture is high at stage A and reduces through stages B to D. The ratio of CDs to PDs is high in early stage B, reduces to parity by late stage B and in stage C and increases again in stage D. For the WS strains used, AG03141 would be late in stage B when the culture was first sampled (PD9) and proceeds to stage C at PD21.5. Therefore the telomere erosion rate is close to the normal range as the cells are growing exponentially (CD $\sim$ PD). For AG00780, the culture is at stage A when initiated and is proceeding from a state with a high number to a state with a low number of clonal lineages (stage C). Thus, the apparent rate of telomere erosion is high initially (CD $\gg$ PD) and then reduces to a normal rate as the culture approaches stage C (CD $\sim$ PD). The AG12795 culture would be in the middle of stage B. AG05229 was possibly at stage A when initiated and approaching stage C at the end of its growth; however, very little data state this conclusively.

senescence (TIS) mechanism. However, as ectopic expression of hTERT is known to immortalize WS cells (24), this TIS mechanism is superimposed upon the normal telomere driven p53-dependent replicative arrest (36). The two mechanisms, working in concert, define the maximum possible lifespan of a WS culture. The actual mechanism of the telomere independent arrest is unknown at this time, although it possibly acts via p53, as it has been shown that abrogation of p53 allows WS cells to bypass senescence and undergo an extended lifespan (36).

Our data also inform about some other aspects of the WS phenotype. The tight distribution of telomere sizes, seen in both clones and the later stages of the bulk WS cultures, suggests that telomere erosion itself is unlikely to be any more heterogeneous than in normal fibroblast strains, despite the known 'mutator' phenotype of WS (13), which a priori

might have predicted an increased level of deletions or rearrangements within the telomere that would lead to a more broadened telomere distribution. Instead, our data are consistent with telomere erosion in WS cells being predominantly a consequence of end-replication losses superimposed with occasional catastrophic telomere deletion similar to that postulated for normal cells (34,45,46). Although only the XpYp telomeres are being analysed in this work, there is no evidence to suggest that the dynamics of the XpYp telomeres observed in this study are not representative of the dynamics of other telomeres in the genome; indeed, previous data demonstrate that it has genetic properties similar to that of three autosomal telomeres (47,48).

Overall, our data provide little support for the *WRN* mutation causing a change in telomere erosion rates as measured per CD; for all four strains, it was possible to produce cultures that, despite the absence of the WRNp helicase, showed normal rates of telomere erosion. Those situations where telomere erosion rates appeared higher showed additional features indicative of a known feature of WS cultures, namely, a tendency to grow in a semi-clonal fashion; this in turn distorts measured telomere erosion rates because the measured PD is no longer an accurate predictor of the number of CDs undergone. The significance of these results is that it suggests that future research into WS should focus on identifying the cause of the slow growth characteristics of WS cells. To this end, it is provocative that WRNp has known interactions with proteins involved in both cell cycle progression, e.g. proliferating cell nuclear antigen (PCNA) and RPA (28,49,50) and signalling pathways that can trigger cell cycle arrest or apoptosis, e.g. p53 (51–53). The interaction between PCNA and WRNp is particularly interesting because PCNA is a potential communication point between a variety of important cellular processes, including cell cycle control, DNA replication, DNA recombination and repair (54). WS cells are hypersensitive to DNA damaging agents (e.g. 4-nitroquinoline-1-oxide) and chemicals that induce inter-strand cross-links such as 8-methoxypsoralen (55–57). Treatment of WS fibroblasts with these agents leads to reduced cell proliferation, but not to p53-dependent apoptosis (57), as the latter is attenuated in WS cells (51). Inter-strand cross-links may be repaired by homologous recombination (58), suggesting that WS cells are deficient in resolving the intermediates of homologous recombination and undertaking the recombinational resolution of stalled replication forks (9). This deficiency leads to a hyper-recombinant phenotype (59,60) and a genomic instability observed in WS that results in an increase in chromosomal aberrations. These data suggest that in WRNp deficient cells there is a decreased ability to ensure genome integrity prior to CD, resulting in a proportion of cells with an induced S-phase arrest or delay. Together, these data suggest that the reduced rate of growth of WS cultures reflects a combination of an increased cell cycle transit time (7–9) and a substantial degree of cell cycle arrest (10).

MATERIALS AND METHODS

Growth of cells

We obtained WS fibroblast cell cultures AG00780, AG03141, AG05229 and AG12795 from the Coriell cell repository. Of these AG00780 (R368X) and AG03141 (Q748X) have defined nonsense mutations in the *WRN* gene, and AG00780, AG03141 and AG05229 have no detectable WRNp by immunoblotting (61,62). Although no *WRN* mutation has yet been reported for AG12795, it has all of the major diagnostic features of WS (Coriell Cell Bank data sheet). Thus, with the exception of AG12795 we have chosen WS cell lines that do not express WRNp. Cells were grown in Dulbecco's modified Eagle's medium (Life Technologies) supplemented with 10% fetal calf serum (Imperial Labs).

DNA synthesis assays

DNA synthesis was assayed by labelling cells in the presence of 10 μM BrdU for 1 h, following which BrdU incorporation was detected as previously described by immunoperoxidase (63).

Infection of WS cells with HPV E6

WS cells were infected with amphotrophic viruses containing the E6 oncoprotein essentially as described (36). To obtain E6-expressing clones with a sufficiently long lifespan for STELA analysis, the infections were done using WS cells at early passage, i.e. using the youngest cells available. Clones at selected PDs were subjected to STELA analysis.

Telomere length analysis

DNA extraction and the determination of XpYp telomere length by STELA were as previously described (34). Genotyping of the −427 and −415 XpYp telomere-adjacent polymorphic sites was as previously described (35).

ACKNOWLEDGEMENTS

We would like to thank members of our laboratories for their discussions. This work was supported by Research Into Ageing (RIA) and the BBSRC Experimental Research on Ageing initiative.

REFERENCES

1. Salk, D. (1982) Werner's syndrome: a review of recent research with an analysis of connective tissue metabolism, growth control of cultured cells, and chromosomal aberrations. *Hum. Genet.*, **62**, 1–5.
2. Goto, M., Miller, R.W., Ishikawa, Y. and Sugano, H. (1996) Excess of rare cancers in Werner syndrome (adult progeria). *Cancer Epidemiol. Biomarkers Prev.*, **5**, 239–246.
3. Martin, G.M., Oshima, J., Gray, M.D. and Poot, M. (1999) What geriatricians should know about the Werner syndrome. *J. Am. Geriatr. Soc.*, **47**, 1136–1144.
4. Brown, W.T., Kieras, F.J., Houck, G.E., Jr, Dutkowski, R. and Jenkins, E.C. (1985) A comparison of adult and childhood progerias: Werner syndrome and Hutchinson–Guildford progeria syndrome. *Adv. Exp. Med. Biol.*, **190**, 229–244.
5. Martin, G.M., Sprague, C.A. and Epstein, C.J. (1970) Replicative life-span of cultivated human cells. *Lab. Invest.*, **23**, 86–92.
6. Fujiwara, Y., Higashikawa, T. and Tatsumi, M. (1977) A retarded rate of DNA replication and normal level of DNA repair in Werner's syndrome fibroblasts in culture. *J. Cell. Physiol.*, **92**, 365–374.
7. Takeuchi, F., Hanaoka, F., Goto, M., Yamada, M. and Miyamoto, T. (1982) Prolongation of S phase and whole cell cycle in Werner's syndrome fibroblasts. *Exp. Gerontol.*, **17**, 473–480.

8. Poot, M., Hoehn, H., Runger, T.M. and Martin, G.M. (1992) Impaired S-phase transit of Werner syndrome cells expressed in lymphoblastoid cells lines. *Exp. Cell Res.*, **202**, 267–273.
9. Rodríguez-López, A.M., Jackson, D.A., Iborra, F. and Cox, L.S. (2002) Asymmetry of DNA replication fork progression in Werner's syndrome. *Aging Cell*, **1**, 30–39.
10. Faragher, R.G.A., Kill, I.R., Hunter, J.A., Pope, F.M., Tannock, C. and Shall, S. (1993) The gene responsible for Werner syndrome may be a cell division 'counting' gene. *Proc. Natl Acad. Sci. USA*, **90**, 12030–12034.
11. Hoehn, H., Bryant, E.M., Au, K., Norwood, T.H., Boman, H. and Martin, G.M. (1975) Cytogenetics of Werner's syndrome cultured skin fibroblasts. *Cytogenet. Cell Genet.*, **15**, 282–298.
12. Salk, D., Au, K., Hoehn, H. and Martin, G.M. (1981) Cytogenetics of Werner's syndrome cultured skin fibroblasts: variegated translocation mosaicism. *Cytogenet. Cell Genet.*, **30**, 92–107.
13. Fukuchi, K., Martin, G.M. and Monnat, R.J., Jr (1989) Mutator phenotype of Werner syndrome is characterised by extensive deletions. *Proc. Natl Acad. Sci. USA*, **86**, 5893–5897.
14. Meyn, M.S. (1997) In Kastan, M.B. (ed.), *Genetic Instability and Tumorigenesis*. Springer, Berlin, pp. 71–148.
15. Hayflick, L. and Moorhead, P.S. (1961) The serial cultivation of human diploid cell strains. *Exp. Cell Res.*, **25**, 585–621.
16. Oshima, J., Campisi, J., Tannock, T.C. and Martin, G.M. (1995) Regulation of *c*-fos expression in senescing Werner syndrome fibroblasts differs from that observed in senescing fibroblasts from normal controls. *J. Cell. Physiol.*, **162**, 277–283.
17. Schulz, V.P., Zakian, V.A., Ogburn, C.E., McKay, J., Jarzebowicz, A.A., Edland, S.D. and Martin, G.M. (1996) Accelerated loss of telomere repeats may not explain accelerated replicative decline in Werner syndrome cells. *Hum. Genet.*, **97**, 750–754.
18. Bodnar, A.G., Ouellette, M., Frolkis, M., Holt, S.E., Chiu, C.P., Morin, G.B., Harley, C.B., Shay, J.W., Lichtsteiner, S. and Wright, W.E. (1998) Extension of life span by introduction of telomerase into normal human cells. *Science*, **279**, 349–352.
19. Vaziri, H. and Benchimol, S. (1998) Reconstitution of telomerase activity in normal human cells leads to elongation of telomeres and extended reproductive life span. *Curr. Biol.*, **8**, 279–282.
20. Forsyth, N.R., Evans, A.P., Shay, J.W. and Wright, W.E. (2003) Developmental differences in the immortalization of lung fibroblasts by telomerase. *Aging Cell*, **2**, 235–243.
21. O'Hare, M.J., Bond, J., Clarke, C., Takeuchi, Y., Atherton, A.J., Berry, C., Moody, J., Silver, A.R., Davies, D.C., Alsop, A.E. *et al.* (2001) Conditional immortalization of freshly isolated human mammary fibroblasts and endothelial cells. *Proc. Natl Acad. Sci. USA*, **98**, 646–651.
22. Ouellette, M.M., McDaniel, L.D., Wright, W.E., Shay, J.W. and Schultz, R.A. (2000) The establishment of telomerase-immortalised cell lines representing human chromosome instability syndromes. *Hum. Mol. Genet.*, **9**, 403–411.
23. Choi, D., Whittier, P.S., Oshima, J. and Funk, W.D. (2001) Telomerase expression prevents replicative senescence but does not fully reset mRNA expression patterns in Werner syndrome cell strains. *FASEB J.*, **15**, 1014–1020.
24. Wyllie, F.S., Jones, C.J., Skinner, J.W., Haughton, M.F., Wallis, C., Wynford-Thomas, D., Faragher, R.G.A. and Kipling, D. (2000) Telomerase prevents the accelerated ageing of Werner syndrome fibroblasts. *Nat. Genet.*, **24**, 16–17.
25. Yu, C.E., Oshima, J., Fu, Y.H., Wijsman, E.M., Hisama, F., Alisch, R., Matthews, S., Nakura, J., Miki, T., Ouais, S. *et al.* (1996) Positional cloning of the Werner's syndrome gene. *Science*, **272**, 258–262.
26. Huang, S., Li, B., Gray, M.D., Oshima, J., Mian, I.S. and Campisi, J. (1998) The premature ageing syndrome protein, WRN, is a $3' \rightarrow 5'$ exonuclease. *Nat. Genet.*, **20**, 114–116.
27. Shen, J.-C. and Loeb, L.A. (2001) Unwinding the molecular basis of the Werner syndrome. *Mech. Ageing Dev.*, **122**, 921–944.
28. Opresko, P.L., von Kobbe, C., Laine, J.P., Harrigan, J., Hickson, I.D. and Bohr, V.A. (2002) Telomere-binding protein TRF2 binds to and stimulates the Werner and Bloom syndrome helicases. *J. Biol. Chem.*, **277**, 41110–41119.
29. Fry, M. and Loeb, L.A. (1999) Human Werner syndrome DNA helicase unwinds tetrahelical structures of the fragile X syndrome repeat sequence $d(CGG)_n$. *J. Biol. Chem.*, **274**, 12797–12802.
30. Kamath-Loeb, A.S., Loeb, L.A., Johansson, E., Burgers, P.M.J. and Fry, M. (2001) Interactions between the Werner syndrome helicase and DNA polymerase delta specifically facilitate copying of tetraplex and hairpin structures of the $d(CGG)_n$ trinucleotide repeat sequence. *J. Biol. Chem.*, **276**, 16439–16446.
31. Monaghegh, P., Karow, J.K., Brosh, R.M., Jr, Bohr, V.A. and Hickson, I.D. (2001) The Bloom's and Werner's syndrome proteins are DNA structure specific helicases. *Nucl. Acids Res.*, **29**, 2843–2849.
32. Ostler, E.L., Wallis, C.V., Sheerin, A.N. and Faragher, R.G.A. (2002) A model for the phenotypic presentation of Werner's syndrome. *Exp. Gerontol.*, **37**, 285–292.
33. Tahara, H., Tokutake, Y., Maeda, S., Kataoka, H., Watanabe, T., Satoh, M., Matsumoto, T., Sugawara, M., Ide, T., Goto, M. *et al.* (1997) Abnormal telomere dynamics of B-lymphoblastoid cell strains from Werner's syndrome patients transformed by Epstein–Barr virus. *Oncogene*, **15**, 1911–1920.
34. Baird, D.M., Rowson, J., Wynford-Thomas, D. and Kipling, D. (2003). Extensive allelic variation and ultrashort telomeres in senescent human cells. *Nat. Genet.*, **33**, 203–207.
35. Baird, D.M., Jeffreys, A.J. and Royle, N.J. (1995) Mechanisms underlying telomere repeat turnover, revealed by hypervariable variant repeat distribution patterns in the human Xp/Yp telomere. *EMBO J.*, **14**, 5433–5443.
36. Davis, T., Singhrao, S.K., Wyllie, F.S., Haughton, M.F., Smith, P.J., Wiltshire, M., Wynford-Thomas, D., Jones, C.J., Faragher, R.G.A. and Kipling, D. (2003) Telomere-based proliferative lifespan barriers in Werner-syndrome fibroblasts involve both p53-dependent and p53-independent mechanisms. *J. Cell Sci.*, 116, 1349–1357.
37. Bond, J.A., Haughton, M.F., Rowson, J.M., Smith, P.J., Gire, V., Wynford-Thomas, D. and Wyllie, F.S. (1999) Control of replicative life span in human cells: barriers to clonal expansion intermediate between M1 senescence and M2 crisis. *Mol. Cell. Biol.*, **19**, 3103–3114.
38. Filatov, L., Golubovskaya, V., Hurt, J.C., Byrd, L.L., Phillips, J.M. and Kaufmann, W.K. (1998) Chromosomal instability is correlated with telomere erosion and inactivation of G2 checkpoint function in human fibroblasts expressing human papillomavirus type 16 E6 oncoprotein. *Oncogene*, **16**, 1825–1838.
39. Stoppler, H., Hartmann, D.P., Sherman, L. and Schlegel, R. (1997) The human papillomavirus type 16 E6 and E7 oncoproteins dissociate cellular telomerase activity from the maintenance of telomere length. *J. Biol. Chem.*, **272**, 13 332–13 337.
40. Schonberg, S., Niermeijer, M.F., Bootsma, D., Henderson, E. and German, J. (1984) Werners syndrome—proliferation *in vitro* of clones of cells bearing chromosome translocations. *Am. J. Hum. Genet.*, **36**, 387–397.
41. Benn, P.A. (1985) Chromosome translocations in fibroblast-cultures derived from patients with Werner's syndrome. *Am. J. Hum. Genet.*, **37**, 221–223.
42. Melcher, R., von Golitschek, R., Steinlein, C., Schindler, D., Neitzel, H., Kainer, K., Schmid, M. and Hoehn, H. (2000) Spectral karyotyping of Werner syndrome fibroblast cultures. *Cytogenet. Cell Genet.*, **91**, 180–185.
43. Littlefield, L.G. and Mailhes, J.B. (1975) Observations of *de novo* clones of cytogenetically aberrant cells in primary fibroblast cell strains from phenotypically normal women. *Am. J. Hum. Genet.*, **27**, 190–197.
44. Benn, P.A. (1977) Population kinetics of chromosomally abnormal fibroblast sub-populations. *Cytogenet. Cell Genet.*, **19**, 137–144.
45. Rubelj, I. and Vondracek, Z. (1999) Stochastic mechanism of cellular aging-abrupt telomere shortening as a model for stochastic nature of cellular aging. *J. Theor. Biol.*, **197**, 425–438.
46. Tan, Z. (1999) Telomere shortening and the population-size dependency of the life span of human cell culture: further implication for two proliferation-restricting telomeres. *Exp. Gerontol.*, **34**, 831–842.
47. Baird, D.M., Coleman, J., Rosser, Z.H. and Royle, N.J. (2000) High levels of sequence polymorphism and linkage disequilibrium at the telomere of 12q: implications for telomere biology and human evolution. *Am. J. Hum. Genet.*, **66**, 235–250.
48. Coleman, J., Baird, D.M. and Royle, N.J. (1999) The plasticity of human telomeres demonstrated by a hypervariable telomere repeat array that is located on some copies of 16p and 16q. *Hum. Mol. Genet.*, **8**, 1637–1646.
49. Lebel, M., Spillare, E.A., Harris, C.C. and Leder, P. (1999) The Werner syndrome gene product co-purifies with the DNA replication complex and interacts with PCNA and topoisomersase I. *J. Biol. Chem.*, **274**, 37795–37799.

50. Huang, S., Beresten, S., Li, B., Oshima, J., Ellis, N.A. and Campisi, J. (2000). Characterization of the human and mouse WRN $3' \rightarrow 5'$ exonuclease. *Nucl. Acids Res.*, **28**, 2396–2405.
51. Spillare, E.A., Robles, A.I., Wang, X.W., Shen, J.-C., Yu, C.E., Schellenberg, G.D. and Harris, C.C. (1999) p53-mediated apoptosis is attenuated in Werner syndrome cells. *Genes Dev.*, **13**, 1355–1360.
52. Blander, G., Zalle, N., Leal, J.F., Bar-or, R.L., Yu, C.E. and Oren, M. (2000) The Werner syndrome protein contributes to induction of p53 by DNA damage. *FASEB J.*, **14**, 2138–2140.
53. Brosh, R.M., Jr, Karmakar, P., Sommers, J.A., Yang, Q., Wang, X.W., Spillare, E.A., Harris, C.C. and Bohr, V.A. (2001) p53 modulates the exonuclease activity of Werner syndrome protein. *J. Biol. Chem.*, **276**, 35093–35102.
54. Jonsson, Z.O. and Hubscher, U. (1997) Proliferating cell nuclear antigen: more than a clamp for DNA polymerases. *Bioessays*, **19**, 967–975.
55. Prince, P.R., Ogburn, C.E., Moser, M.J., Emond, M.J., Martin, G.M., and Monnat, R.J., Jr (1999) Cell fusion corrects the 4-nitroquinoline 1-oxide sensitivity of Werner syndrome fibroblast cell lines. *Hum. Genet.*, **105**, 132–138.
56. Hisama, F.M., Chen, Y.-H., Meyn, M.S., Oshima, J. and Weissman, S.M. (2000) WRN or telomerase constructs reverse 4-nitroquinoline 1-oxide sensitivity in transformed Werner Syndrome fibroblasts. *Cancer Res.*, **60**, 2372–2376.
57. Poot, M., Gollahon, K.A., Emond, M.J., Silber, J.R. and Rabinovitch, P.S. (2002) Werner syndrome diploid fibroblasts are sensitive to 4-nitroquinoline-*N*-oxide and 8-methoxypsoralen: implications for the disease phenotype. *FASEB J.*, **16**, 757–758.
58. Hoeijmakers, J.H. (2001) Genome maintenance mechanisms for preventing cancer. *Nature*, **411**, 366–374.
59. Cheng, R.Z., Murano, S., Kurz, B. and Shmookler Reis, R.J. (1990) Homologous recombination is elevated in some Werner-like syndromes but not during normal *in vitro* or *in vivo* senescence of mammalian cells. *Mutat. Res.*, **237**, 259–269.
60. Elli, R., Chessa, L., Antonelli, A., Petrinelli, P., Ambra, R. and Marcucci, L. (1996) Effects of topoisomerase II inhibition in lymphoblasts from patients with progeroid and 'chromosome instability' syndromes. *Cancer Genet. Cytogenet.*, **87**, 112–116.
61. Marciniak, R.A., Lombard, D.B., Johnson, F.B. and Guarente, L. (1998) Nucleolar localization of the Werner syndrome protein in human cells. *Proc. Natl Acad. Sci. USA*, **95**, 6887–6892.
62. Grandori, C., Wu, K.J., Fernandez, P., Ngouenet, C., Grim, J., Clurman, B.E., Moser, M.J., Oshima, J., Russell, D.W., Swisshelm, K. *et al.* (2003) Werner syndrome protein limits MYC-induced cellular senescence. *Genes Dev.*, **17**, 1569–1574.
63. Bond, J., Haughton, M., Blaydes, J., Gire, V., Wynford-Thomas, D. and Wyllie, F. (1996) Evidence that transcriptional activation by p53 plays a direct role in the induction of cellular senescence. *Oncogene*, **13**, 2097–2104.